Research Article

Art Valta*, Mika Ruusunen, and Kauko Leiviskä

On-line moisture content estimation of saw dust via machine vision

https://doi.org/10.1515/eng-2020-0035
Received Aug 15, 2019; accepted Feb 03, 2020

Abstract: The effect of moisture content and feasibility of its estimation in granular material was investigated via machine vision. The test scheme consisted of saw dust samples derived from Norway spruce with moisture content adjusted to three distinct levels. The effect of moisture when present as ice or liquid water was compared. The experimental procedure consisted of pouring the saw dust under video camera recording. The equipment setup consisted of a vibrator feeder and custom-built pouring frame. Still images were extracted with fixed sample time from the recording done during the pouring procedure. From the extracted frames the dynamic behavior of cone profile was investigated via statistical means. It was observed that 2nd standardized moment correlated with moisture content, phase of water and their interaction. Furthermore, 4th standardized moment correlated with moisture content and phase. The 3rd moment was inspected qualitatively from which it was observed that wet samples exhibited tendency to build mass accumulation sites with increasing moisture content. Samples where water was present as ice this was observed in a very small scale with all moisture content values. Corroborated by optical microscopy, these correlations were deduced to be due to liquid bridging in the bulk. Moisture content when present as ice was, however, observed to have a drastic effect on the overall cone shape. Based on these findings, a machine vision application could be feasible way to estimate moisture content on-line in thawed saw dust by using statistical parameters in classification decision making. This would enable cost-effective on-line monitoring of moisture content and a control circuit to be designed.

Keywords: sawdust, moisture content, angle of repose, estimation

***Corresponding Author: Art Valta:** Control Engineering, Environmental and Chemical Engineering, University of Oulu, P.O. Box 4300, 90014 Oulu, Finland; Email: art.valta@student.oulu.fi
Mika Ruusunen, Kauko Leiviskä: Control Engineering, Environmental and Chemical Engineering, University of Oulu, P.O. Box 4300, 90014 Oulu, Finland

1 Introduction

Due to ever more present climate considerations in the industry, alternative sources of raw materials are sought to diminish the dependence on the fossil sources. Especially intriguing sources of raw materials are those which currently possess little or no economic value and are abundantly available. The by-products of forest industry are available in large quantities in Finland and wood chips have a proven value as a raw material even today. Today also saw dust, the finer fraction of wood residues, is gaining attention in the industrial scale.

One of the research directions currently present seeks to find methods to utilize saw dust in biofuel production [1]. A significant challenge in the use of saw dust is its unique flowability properties, similar to other granular materials. The motion is governed by microscale interactions between individual particles and surrounding fluid medium. The physical properties like size, shape and moisture content of the particles also contribute to motion [2]. The shape has been argued to be function of size to which granular is material is produced and the structure of wood [3]. The moisture content is important factor also when processing is concerned. Variation in moisture content brings up disturbances during the processing and needs to be controlled to achieve uniform operating conditions [4]. Furthermore, the biological nature of saw dust brings about variations to physical properties, like the moisture content [5].

Most of the pre-existing methods for measuring the moisture content have too long procedural times with respect to the variation of the moisture content in the feed scales of industrial plant. A good example of such slow procedure is the moisture content measurement by oven drying. The industrially viable on-line sensors are almost exclusively based on electromagnetic radiation, the most popular being arguably the near-infrared radiation spectroscopy and radio frequency methods [6]. The drawbacks of these need for calibration to specific raw-material and complex interpretability of raw data from which the estimates are produced [7–9]. A device capable of on-line mon-

itoring with easy interpretability and generalizability with respect to raw material would be of great use.

With these challenges in mind, this work sought to investigate whether the intrinsic macroscopic behavior of the saw dust could be used to infer moisture and possibly other relevant properties regarding to flowability. A well-known and easily observable property of granular material is its tendency to form a heap when let to flow under gravity. The heap and its flowing properties are usually characterized by its angle that is formed between the heap surface and the horizontal line [10]. Its usage, however, with materials where cohesive interactions are present is not particularly informative. This is due to the non-uniform heap formation; the heap side will not be smooth and may not even be straight which is required for angle of repose to have any meaning [11]. Still, the angle of repose is many times approximated as the plain inverse tangent of the ratio of heap height and radius, implicitly assuming the side of heap being straight and smooth [12].

It has been observed that moisture contributes in a cohesive manner between objects [13]. When particle size decreases, the magnitude of cohesion increases relatively [14]. The source of liquids' cohesive contribution is due to liquid bridging or capillary force [15]. Because the cohesion gives rise to deviations in the heap formation, it is then logical to ask, if these deviations contain some useful information about its source. In this work the angle of repose and the deviations the heap exhibit from it were used as data to infer moisture content in the sample. The aim was to find the features, which manage to explain the moisture levels in an adequate manner. In the following sections the theoretical basis upon which inference was built is presented. Pictures of particle assemblies are given to proof existence of phenomena on the basis of theory. Sample preparation, the experimental set-up along with data analysis are reported to assert that the proposed of method is sound and the results are valid.

2 Theory of cohesion via liquid water

The cohesiveness is typically a function of particle dimension. This is observed to hold true also in wood substances with shape also having an effect [16]. A typical source of cohesion of this kind are Van der Waals forces. When liquid is present, the effect of its tendency to form bridges between particles dominates over these forces [17]. The source of cohesion then becomes the liquid water and its interactions in the granular material.

The role of liquid as a source of cohesion is not a simple one, rather, many parameters affect its magnitude. When liquid is water, one of the important factors are the rate of strain and the features of interfacial liquid water between particles. When the rate of strain is low and static configurations are considered, interfacial liquid water becomes a dominant contributor. The effect of moisture is known to depend also on the granular materials' particle parameters [18].

Althaus & Windhab [19] classified liquid water in granular material into three groups based on its interfacial features; the pendular, funicular and capillary states. In the pendular state the bridges exist only between two particles. In funicular state regions of liquid water can be observed in addition to bridges. These regions are bound by air-liquid water surface interfaces which are spanned by a group of particles. In capillary state the void space between particle assembly is mostly occupied by liquid water and only large regions of liquid water exist. The factor determining the state is a function of liquid water content, the fraction of liquid water in the void between particles.

The interfacial liquid water and its contribution to the static case has been studied via simulation by Delenne *et al.* [20]. Liquid water content is defined as ratio between the volume of liquid water and volume of the available space between particles. The results characterize the pendular state to exist below 30% liquid water content. Funicular state exists between 30% and 50% and above this the state there is a liquid water-soaked space with distinct air bubbles. This is what can be referred to as the capillary state [20].

When the behavior of liquid water is discussed in wooden substances it is important to point out that the liquid water, which actually is located in the void space between the particles count towards the liquid water content. Liquid water can also be bound to wood fibers and into the void spaces inside the particles. Liquid water bound to fibers via intermolecular forces is referred as bound liquid water and liquid water residing in the lumina and cavities is referred as free liquid water. When fibers of wood are saturated with liquid water – no more liquid water could be added as bound liquid water – this moisture content is referred to as fiber saturation point. Fiber saturation point is reported to be species specific, but variability between individual trees may be present. Fiber saturation moisture content is many times assumed to be residing at 23%, wet basis [5]. Wet basis – w.b – is defined via equation

$$\text{w.b} = \frac{m_{H_20}}{m_{dry} + m_{H_2O}} \tag{1}$$

where m_{H_2O} refer to the mass of liquid water in sample and m_{dry} to the mass of sawdust when it contains no liquid water. The liquid water hold-up capacity inside the particle is dependent on the porosity of the wood and the liquid water's capability to access the pores. Liquid water is able to occupy diameters down to 1.8 nm in wood. Porosity is defined as

$$\mathrm{n} = 1 - \frac{\rho}{\rho_s} \tag{2}$$

where n is the porosity, ρ the density of oven dry wood and ρ_s as the cell wall density. Norway spruce total porosity was reported to be 74% of which micropores that are possibly inaccessible by liquid water because of size limitation is less than 5% [21]. This is consistent with the fact that softwoods are built up largely from tracheid cells, which have large luminal space inside the fibrous cell wall [22].

Finally, the properties of wood fibers of cell wall have been researched by Stasiak *et al.* [23]. They measured saw dust's flowability properties and cohesiveness as a function of consolidation stress. Observations included that the modulus of elasticity decreased significantly in saw dust with rising moisture content from 10% to 50%.

3 Materials & Methods

3.1 Sample preparation and experimental design

Batch of Norway spruce saw dust was used as a raw material for samples. The saw dust is the residue of a sawmill situated in northern Finland. A batch of saw dust approximately 30 kg was first sieved by 4mm sieve. Then the sample was run through halving apparatus so that sample was first divided into two fractions, these again to two fractions separately and so on until 16 samples were obtained. By assumption of the working principle of the halving apparatus, this procedure conserved the particle size and shape distributions of the original batch sample. Of these three samples were retained for the purposes of this work and stored into polypropylene buckets. The samples were left to dry in an oven set to 60°C. The drying procedure was continued up to point where the ratio of lost mass to the original mas diminished to 1% when the measurement interval was 24h. The drying procedure took eight days to reach this point.

After the drying the levels of moisture were adjusted to 20%, 45% and 60%, w.b, with three adjusted samples for each moisture content. These levels were labelled as low, intermediate and high, respectively. The liquid water was added to buckets of samples by measuring beaker. After this the buckets were sealed by duct tape and placed into oven set to 60°C for one week. The buckets were vibrated daily to facilitate moisture diffusion between particles.

The experimental design to evaluate the effect of moisture content and phase of liquid water was of full factorial type, with three levels for moisture content and two levels for the phase of water. The design incorporated three replications, amounting to 18 test procedures in total.

3.2 Pouring and measurement system

According to Al-Hashemi *et al.* [24] the dependence of the angle of repose on granular materials with respect to physical properties can be amounted to

1. angle of internal friction,
2. grain size,
3. shape,
4. density,
5. moisture content – MC.

Furthermore, angle of repose is dependent also on the method of pouring. Many methods of pouring exist as reported by Geldart *et al.* [25]. To eliminate the contribution of both sources, the material needs to be homogenized with respect to material parameters and the pouring set-up needs to be specified beforehand with respect to pertinent variables. This work uses a fixed funnel type set-up. According to Al-Hashemi *et al.* [24], the dependence of the angle of repose with respect to parameters of pouring technique are

1. Roughness of the base,
2. Segregation,
3. Mass of the poured material,
4. Pouring height.

The pouring height depicts collectively the contribution that falling particles inertia has on the angle of repose increasing compressive stress at the tip region of the heap. Thus, the pouring height should be treated as to also cover material flow. It is noted that the listing of the variables should be interpreted as contributions of granular material when considered as dry. The density of the particles is affected by moisture content, for example. Finally, in order to quantify moisture's effect on the angle of repose, in addition to homogenizing the samples, also the method of pouring should be fixed with respect to these variables. The pouring procedure should be done under steady state which here means that all reported variables affecting the AOR stay constant during pouring. Also, the average cone

height shall not evolve over time and temperature of the surroundings stay constant.

As the presence of liquid brings about random deviations from the ideal case of straight side heap, it seems logical to treat the heap as a process stochastic. This implies then that measurements done at any instant are meaningless and many measurements over time should be taken. The extraction of the data should be done swiftly with minimal bias and several times to every sample. With these requirements, the most suitable choice for conducting measurements was determined to be a video camera with data extraction being done algorithmically using techniques that come from machine vision.

The experimental procedure was designed according to some heuristic guidelines:

1. The only moving part during procedure is the feeder
2. All other sources of variation in the heap formation are eliminated
3. The dimensions of the poured heaps need to be comparable to each other
4. Once procedure is initiated, observer's interaction should be minimized, if not entirely absent
5. The interpretation of data should be made easy and computationally fast

To make data readily available from the video material, a distinctive marker feature was placed onto the investigated heap. This was achieved by a laser source. The contrast between the color of the laser and the surroundings should be maximized. This was achieved by minimal ambient lighting and black covering of the experimental frame. The laser source wavelength was 635 nm, which in RGB coding corresponds to the peak in red channel, and 0 in others. This turned out to be adequate setting to extract heap side from the still images with simple thresholding.

The frame used consisted of a holder for the video camera and the laser source, a fixed height polypropylene funnel and a circular pouring plate made from cross-laminated timber with 15 cm radius. Funnel outlet was fixed to height of 22 cm with funnel length 15 cm. A schematic illustration of the apparatus is given by Figure 1. The funnel was fed by saw dust from above via vibrator feeder. To make pouring height uniform, the feed was aimed into the funnel so that no particles entered the funnel tube directly but collided with the surface of the funnel inlet before entering the tube. The pouring plate was circular so that the poured heap assumes roughly a shape of a circular cone.

To make the cones comparable with each other, a universal length scale needs to be used. It is evident that measurements of height and length keep growing as a function

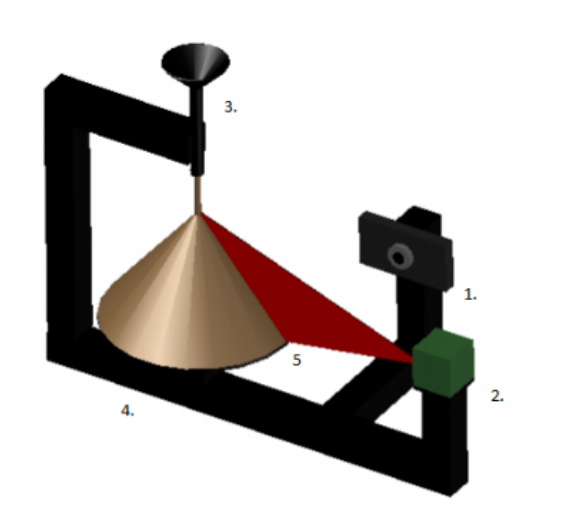

Figure 1: The test apparatus. Parts included: 1. Video recorder, 2. Laser source, 3. Funnel, 4. Pouring plate, 5. feature marker.

of pouring time. To circumvent this, the feeder plate was elevated 10 cm off the base. This way as the poured cone's base reaches the perimeter of the feeder plate, the inflow of mass is either deposited as increased height of the cone or as an outflow across the perimeter. From this point onward, the radius of the cone stays constant. This assures comparability of pouring procedures with respect to dimensions because radius stays constant across the poured heaps. In Figure 1 the pouring has reached the perimeter of the plate, while in Figure 2 the pouring is still developing towards the perimeter.

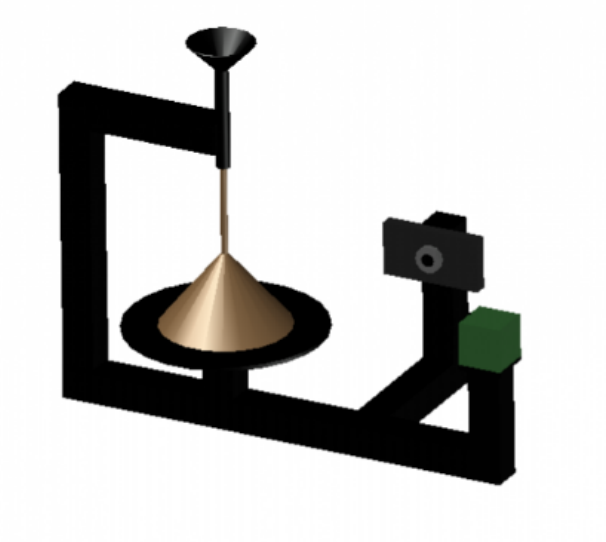

Figure 2: The growth of cone towards the perimeter.

The flow rate of material was fixed by predetermining an amplitude for vibrational feeder achieving the desired rate. The rate was constrained so that the sample level having the worst flow properties did not exhibit consistent arching. The arching could not be eliminated wholly in any sample levels as a random placement of needle shaped dust particles was able to clog the funnel. During pouring procedure if this occurred, the vibrating machine was turned off, upper part of the funnel was removed from the frame, cleaned and reinstalled into frame. With these considerations, the flow rate was set to 2.2 cm^3/s. The actual duration of the pouring procedure was recorded.

With the described set-up the heuristic guidelines mentioned above are fulfilled and, by assumption, the observer's interaction with the experimental pouring procedure is minimized. Any source of variation in the AOR would then be due to moisture content. The physical properties are fixed with specification given in sections 3.1 and 3.2. Specifically, angle of internal friction and density are material properties. These are fixed because saw dust from a specified unique source is specified in section 3.1 Grain size and shape along with their distributions in samples are uniform and thus fixed on the basis of halving procedure specified in section 3.1. The pouring procedure dependent parameters relating to AOR are fixed in an adequate manner because base plate material stays constant along with the pouring height as described in section 3.2. Mass of material cannot be assumed constant. However, as volumetric flow of dust is assumed constant by arguments given in section 3.2, only the density affects mass to be poured. Because physical properties are fixed apart from moisture content, the variation of density can be incorporated to the changes in moisture content. Because inferencing target is the moisture content, the nature of this variation is acceptable. Neither can the segregation be assumed to behave in a uniform manner across the sample levels since density might have indirect contribution to this effect. However, with similar arguments as with the poured mass, density is the only source of variation with segregation, the moisture content may be deduced to be the source of variation. Again, this variation is then acceptable as the moisture content is the target of inferencing.

3.3 Pouring procedure

The pouring was initiated by ensuring the horizontal levelling of the feeder plate and vertical levelling of the funnel tube. The frozen samples were placed in a freezer operating at −20°C. The sample was mixed in the storage bucket after which the vibrating feeder's storage container was filled with the saw dust. The predetermined vibrating amplitude was set, and the feeder switched on. With frozen samples, the remaining unloaded fraction of saw dust was placed back to freezer. The container was filled if needed.

After the poured sample once had reached the perimeter of the pouring plate, the vibrating feeder had its storage container filled full once again. After this the container was let to run empty. At this point the cone was assumed to reach the steady state; cone shape and height stayed constant on average. After this the vibrating feeder was filled half-way, the video camera was installed on the holder and procedure was let to proceed. The time target of this recorded stage from start to completion was 15 minutes according to the predetermined flow rates. The pouring apparatus was located with surroundings with temperature approximately 20°C. The pouring of different samples was randomized to eliminate bias of any possible external action.

3.4 Data preparation

The still images were extracted from the recorded video material with framerate ratio 1:10. This corresponded to sampling time of approx. 0.3 seconds. Any footage which involved arching at the funnel was deleted. After this, to ensure the steady state assumption of the material, only the last 1813 frames were used for analysis. This amount corresponded to roughly 10 minutes of footage. Figure 3. shows an example of an extracted image from the footage with the feature marker clearly visible.

Figure 3: Example of extracted image from recorded footage.

The extracted feature marker from each image was converted to data points by defining a matrix coinciding with the dimensions of the pixel grid of the images. To make all pictures equally weighted, only one pixel as a function of radius was chosen from each image. The de-

cision criteria for this pixel was determined to be the pixel with minimum height sharing the same radius coordinate. This guarantees somewhat uniform contribution of each image to the raw data. If multiple pixels could be chosen from any one image, the bias would be towards the images that had very thick occurrence of the feature marker.

The chosen pixels from image were then converted to data points simply by assigning the marker feature pixel to the coordinates of the matrix that corresponded the pixel's location in the still image. The marker feature pixels from all 1813 still images were gathered to this matrix by summing up all the feature marker pixels with same coordinates in the matrix positions. Figure 4 shows the plot of the image presented in Figure 3 as the extracted data points placed onto blank data matrix.

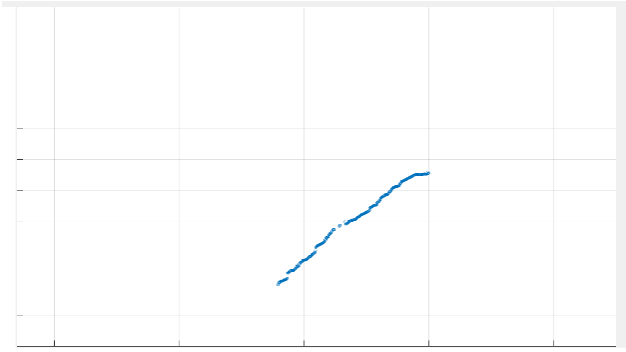

Figure 4: Extracted marker feature pixels from example image stored to data matrix.

Finally, Figure 5 shows an example plot of collection of images whose data points have been stored onto the data matrix.

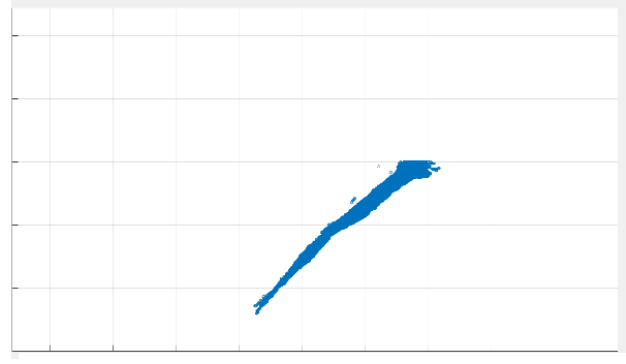

Figure 5: Extracted marker feature pixels from 1000 example images stored to data matrix.

3.5 Data analysis – feature selection, regression

The obtained data matrix serves as a storage of distributions of random variables as a function of height. Each height corresponds to all occurrences of marker feature pixels that occurred at this height. Thus, it can be said that with the given height the location of cones side is a collection of independent, identically distributed random variables with certain parameters defining the distribution.

To make inferences about features that can be thought of as distributions, some statistical quantities are a natural way to quantify them. In this work the standardized moments were used. The standardized moments are defined with the formula

$$\mu_n = \frac{E[(X-\mu)^n]}{(E[(X-\mu)^2])^{\frac{n}{2}}} \tag{3}$$

where E denotes the expectation operator, X the random variable, n the order of moment and μ the mean of distribution. The first and second moments are used cumulatively in this work, which are the mean - μ - and variance - σ^2. Skewness – the 3rd moment γ - and kurtosis – the 4th moment κ – are used in standardized form.

In order to quantify the angle of repose of the sample, first order regression is used. The regression finds the best fit of straight line for a collection of means of the distributions obtained as a function of height. Regression used is ordinary least squares method – OLS. This means that the line is fitted to the collections of the means of distributions by minimizing error of residual in the least squares way with equal weight placed between the means. The angle of repose is defined here as

$$\theta = \tan^{-1} \mathrm{k} \tag{4}$$

where k is the first order coefficient of the regression.

In addition to the moments being the mathematical way of expressing the distribution behavior, qualitative argumentation can also be formulated as a research hypothesis. The flow of saw dust cycles between slow accumulation and sudden collapsing phases. In an ideal case, all interactions between particles can be presented by the well-known formula of sliding friction

$$F_{friction} = \mu_{kinetic} \mathrm{mg} \tag{5}$$

where $F_{friction}$ refers to the macroscopically observed force of friction, $\mu_{kinetic}$ is the coefficient of the sliding kinetic friction, m the mass and g the acceleration of gravity. When these stages vanish the flow of grains becomes steady along the cone profile, resulting in a uniform cone.

Because of nonidealities grains get bound with each other and form sites where locally the configuration deviates from the ideal shape. The mass accumulates into these sites. With time, the sites grow larger up to a point where the accumulated mass causes the configuration to fail and a sudden collapse occurs.

The mass builds up until it reaches the critical point after which the mass collapses along the side of the cone. On average the cone would exhibit some simple form of the side profile, straight or maybe somehow curved. The collection of means of the cone's surface measures this profile and is interpretable to angle of repose by first order OLS.

Because of the accumulations and collapses of the cone, the profile exhibit variability as a function of height. The variance is the measure how wide this variability is at given height. The skewness is a measure of the symmetry of the side profile. Positive skewness indicates the distribution having larger fraction of points to the left of the middle point of the distribution. With negative skewness the data points are concentrated to the right of the distribution. The accumulation of saw dust should then be seen as sites of negative skew.

When collapses happen the loss of mass along the cone profile is very sudden. The variance takes into account the average variation that takes place along the cone profile. Most of the time the profile is undergoing the accumulation step after collapse. After the collapse the profile is convex. During accumulation the profile is first set straight and after this point into concave curve. The extent of this behavior is visible with variance but the sudden extreme points occurring at the collapse are obscured into the larger fraction of intermediate variation. The kurtosis reflects the event of "sudden behavior" as it gives very little weight to small and intermediate variation but significant contribution to large deviations from the mean. Figure 6 depicts the sequence of accumulation after which the collapse starts over the cycle.

Figure 6: Convex, straight and concave cone profiles observed during pouring.

The angle of repose is a measure of the cone profile which is governed by the physics of the system. With the hypotheses formulated above it is then assumed that by fixing all other contributions to the angle of repose than the moisture content and its phase, the contributions of these same parameters with respect to overall cone profile and to physics have also been fixed. Thus, any observed correlation between these statistical quantities and OLS determined AOR, which track the properties of the cone profile, is accountable to the varying moisture content and its phase due to the change they cause onto the governing physics.

3.6 Quantitative study – Analysis of variance

In order to assess statistical significance of the experiments, analysis of variance – ANOVA – was computed for the data of 13^{st}, 2^{nd}, and 4^{th} moments. The data sample for ANOVA was constructed from the collection of sample cone profile images converted to data matrix, as described by Fig 5. From this data matrix, the x-values values corresponding to the y-axis values on the interval 251px to 400px was used as raw data for variance and 10px to 150px was used for kurtosis. These intervals corresponded, roughly, to one third of the whole cone height. The middle third was observed to in preliminary work to contain most variance. Likewise, for kurtosis, the lower third was observed in preliminary work to site with sudden collapses. For this data, statistical quantities were calculated for each height value. Then these values were used to draw average value of the statistical quantity across the y-axis interval.

The ANOVA consisted of two-way, two-tailed test with 3 repetitions. The two ways of ANOVA were the moisture content and phase of water. The null hypotheses for all the tests were

$H_{0,1}$: The average value of a statistical quantity with different MC's are the same.

$H_{0,2}$: The average values of a statistical with different phase of water are the same.

$H_{0,3}$: The average values of a statistical quantity with all combinations of MC and phase of water are the same.

Alternative hypotheses were

$H_{a,1}$: At least one level of MC has its statistical quantity's average differing from the other groups.

$H_{a,2}$: At least one level of phase of water has its statistical quantity's average differing from the other groups

$H_{a,3}$: At least one level of the combinations of MC and phase of water has its statistical quantity's average differing from the other groups.

With this type of test, the direct effects of studied variables can be tests along with their interaction; The quantities may behave differently if moisture content and phase of water are changed simultaneously rather than one at the time. The first two hypotheses test the independent effects, and the third the interaction. The significance level – α – was set to 0.05. In this case, for ANOVA to reject null hypothesis, P-values would need to obtain a value 0.025 or lower. The observation associated with this P-value would then be stated as a statistically significant observation.

3.7 Optical microscopy inspection

To obtain a qualitative view of the sites of liquid water in saw dust, optical microscope was used to examine the surfaces of the particles and void space between them. The samples were first poured into the containers following the procedure described in section 3.3 and then frozen. From the frozen heaps surface, a scoop of a size of a teaspoon was extracted onto a microscope slide.

Ideally, to test the hypothesis, the microscopy should be done directly onto the surface of the heap. As this is not physically possible, the method described above was deemed as an acceptable compromise. As the samples were frozen, the assembly of the heap produced by pouring would retain any possible liquid bridges as bridges of ice during scooping because of mechanical rigidity of the ice. When preparate is then let to thaw under a microscope, particles retain the interfaces that would form during the pouring of samples into containers. With the microscope, liquid water on the surface may also be examined. Thus, overall caption of an assembly, which describes the space between particles and any eventual bridges, is essential for evaluating the hypothesis. Moreover, a picture with magnification onto a single particles surface could reveal pertinent information of liquid waters behavior in the assembly even if no bridges would be detected as bound liquid water is also present as stated in section 2.

4 Results & Discussion

Below the P-values of ANOVA is reported to state statistical significance of the study. Furthermore, graphs of calculated statistical quantities are presented for samples with liquid water and ice. The results are reported with the labels assigned to different levels of moisture content in samples as defined in section 3.1. In graphs, the curves represent the means based of the three replications. Here the samples with liquid water as referred as wet and samples with ice as frozen.

4.1 Summary of statistical data

Below the angle of repose, variance and kurtosis are presented for wet and frozen samples in Table 1 and Table 2, respectively. The statistical quantities are reported as the average value across all similar samples and over the whole reported height interval.

Table 1: Wet sample profiles, 13st, 2nd & 4th moments.

MC, Wet	θ	σ^2	κ
Low	46.9	50.4	4.08
Int	45.1	78.2	7.86
High	43.8	207	8.64

Table 2: Frozen sample profiles, 13st, 2nd & 4th moments.

MC,Frozen	θ	σ^2	κ
Low	45.9	52.0	3.81
Int	45.5	50.2	5.93
High	48.6	24.1	5.55

Table 3 summarizes the quantitative analysis of results with associated P-values.

Table 3: P-values summary, 13st, 2nd & 4th moments.

P-values	θ	σ^2	κ
MC	0.446	0.0104	$4.34*10^{-3}$
Phase	0.0643	$5.99*10^{-4}$	0.0246
Interaction	0.043	$6.59*10^{-4}$	0.279

It is seen that AOR is not a statistically significant observation as a function of MC, phase or their interaction. However, it is worth to note that the slope is very sensitive to any offset of the camera. Unfortunately, some tilting offset was observed. This most probably increases the internal variance to such a level, that ANOVA would conclude the null hypothesis as valid. Because of randomized sequence of sample pourings, the internal variance because of the tilt offset should be of similar magnitude in all level classes. Variance has statistically significant dependency

on moisture content, phase and their interaction. Kurtosis has statistically significant dependency on moisture content and phase.

4.2 Cone profiles

Cone profiles of wet and frozen samples are presented in Figure 7 and 8, respectively. The y-axis represents the height and the x-axis the width of the cone.

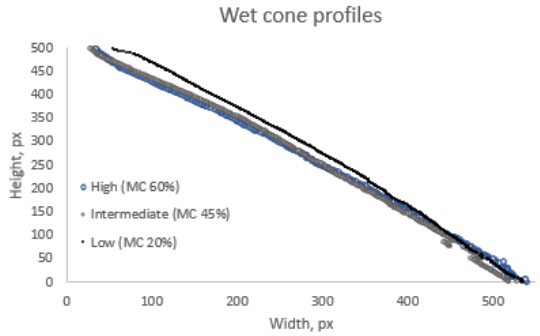

Figure 7: Average wet sample cone profiles.

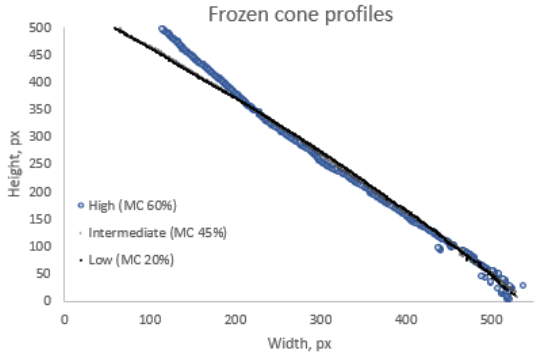

Figure 8: Average frozen sample cone profiles.

Bearing in mind the occurrence of offset described in section 4.1, it is seen that phase and interaction are much close to significance threshold than moisture content. This suggests that moisture content alone will not affect AOR with definite correlation. Any correlation exists with the interaction of phase and Mc, and phase directly. The interaction is something that was observed qualitative; MC was correlating with AOR when phase of water was ice and correlating negatively with AOR when water was present as liquid.

4.3 The variance of cone profiles

The variances - σ^2 - for the poured wet and frozen samples are presented in Figure 9 and 10, respectively. In Figures 9-14 the y-axis represents value of the statistical quantity and the x-axis the height of the cone.

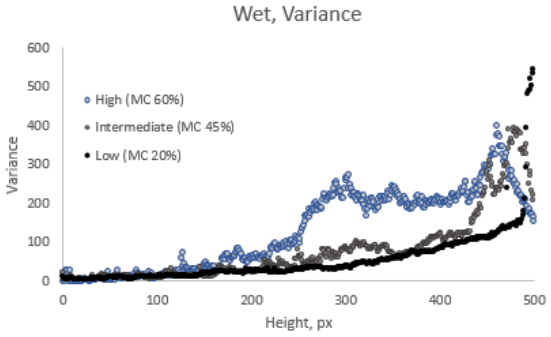

Figure 9: Variances of wet sample profiles.

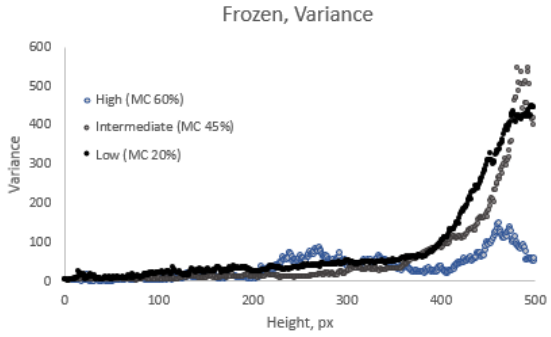

Figure 10: Variances of frozen sample profiles.

The variance as a feature is seen to be statistically significant observation as function MC, phase and their interaction. The P-value of MC is 2 orders of magnitude higher than that of phase and interaction. The interaction is evident as variance correlates with MC when phase of water is liquid and correlates negatively with MC when phase of water is ice. Phase of water is seen to have overall effect on variance as liquid water seems to produce higher variance compared to ice. A cause behind this would be that low samples have surface free of water of any kind. This is reasonable as low samples are approximately at fiber saturation moisture content point. It then seems reasonable that frozen and wet low samples have similar variance values. When water is added the surface is soaked with water or ice. This is the advent of liquid bridging and variance

rises with wet samples. In frozen samples no bridging occurs, and variance stays rather constant. When water is still added, the variance jumps in wet samples because liquid bridging caused cohesion force exponentially grows as suggested by Delenne *et al.* [20]. In frozen samples variance decreases which suggests that ice functions with different mechanism at the interface between particles. The ice may change the surface of particles so that they have tendency to get stuck; particle surface gets rugged producing more rigid structure of the heap.

4.4 Skewness of cone profiles

The skewness - γ – for the poured wet and frozen samples are presented in Figure 11 and 12, respectively.

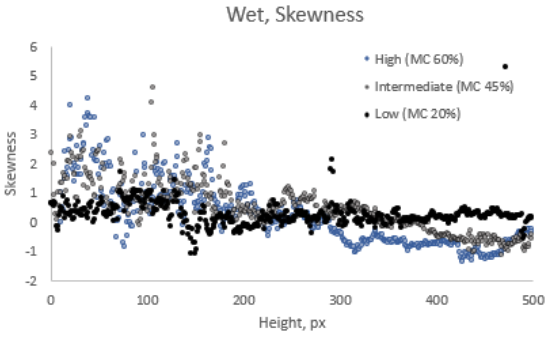

Figure 11: Skewness of wet sample profiles.

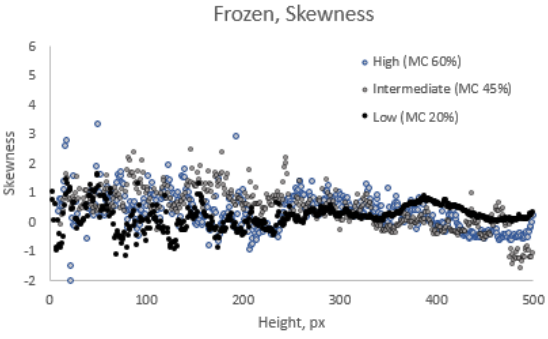

Figure 12: Skewness of frozen sample profiles.

In skewness it is very dubious to assert any correlation with moisture content or phase to exist when average values when calculated as described in section 3.6 are considered because skewness can also obtain negative values. Qualitatively it can still be seen that the skewness tends to decrease as a function of cone height and this rate of decrease is in correlation with moisture content. With frozen samples the skewness this behavior is greatly diminished. This is consistent with the hypothesis that liquid bridges allow the accumulation of mass which then slides down.

4.5 The kurtosis of cone profiles

The kurtosis - κ - of the poured wet and frozen samples are presented in Figure 13 and 14, respectively.

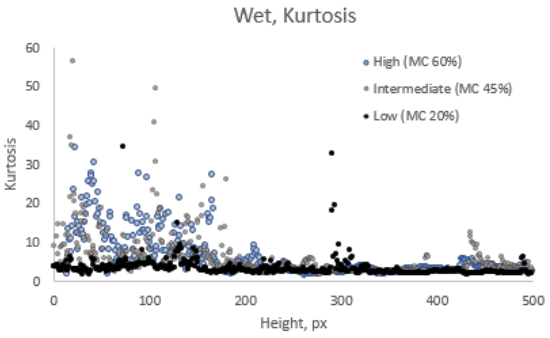

Figure 13: Kurtosis of wet sample profiles.

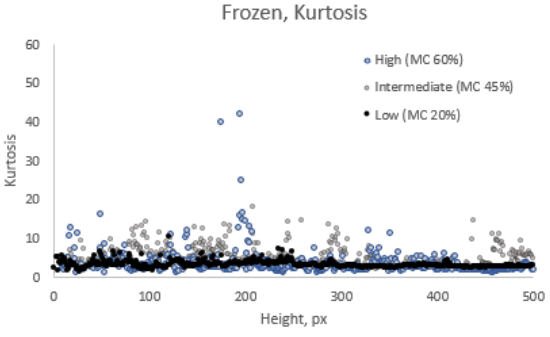

Figure 14: Kurtosis of frozen sample profiles.

The kurtosis is seen to have statistically significant dependency on moisture content, and phase but not on their interaction. Additionally, the null hypothesis of phase dependency is barely rejected. This seems to be in line with the idea that increasing moisture content makes the structure more rigid when water is liquid or ice. In water this may happen because of liquid bridging; sudden extreme collapses near to base are also more frequent when water is present whereas in ice only the sudden extreme collapses govern the dynamic behavior of the heap. When particle

interface contains water, the liquid bridges are not rigid, but allow movement with less restraint compared to ice. When enough mass has accumulated to the top parts of cone, it slowly is deformed so that the base swells. This swelling ends the structure failing, and collapse happens. Ice on the other hand is very rigid as solid and is able to lock particles in place. This way no swelling happens, and there is less mass at risk of collapsing. This decreases the observed kurtosis values. Because the base needs to carry the mass of the top region, eventually the strength of the base reaches a point where the structure fails. Because ice has no bridging present, the failure happens instantly with no slow shifting of mass. The base breaks down all at once. This is consistent with the hypothesis that liquid bridging bounds together the particles but also that ice may have differing mechanism governing the interactions between particles.

4.6 Inspection of particles with optical microscopy

The samples of different moisture content levels are presented in Figs. 15-20. Figure 15 and Figure 16. are the images of the low moisture content level particle sample and its 10-fold magnification onto the surface of a specific particle, respectively. With the same arrangement Figure 17 and Figure 18 represent similar pictures of intermediate moisture content level sample with 2-fold magnification onto a particle surface. Figure 19 is an example of high moisture content. Figure 20 represents the same location and magnification as Figure 19 after the sample was let to thaw under the microscope. In Figures 15-19 the pictures were, in the end, taken before the samples were let to thaw under the microscope because this improved the contrast between the fibers of the particles and liquid water significantly. When samples were let to thaw afterwards, the droplets retained their position and shape. Because of this, taking the images from still frozen samples was deemed as justifiable to obtain the improved contrast.

Qualitatively it can be said that low and intermediate samples do not exhibit liquid bridging to significant extent, rather, the liquid water is bound to the crevices of particle surfaces. Intermediate sample is seen to have somewhat more ice on the surfaces than the low sample. When length scales are compared it is seen that the intermediate sample has visible ice on the surfaces with magnification less than with the low sample. Furthermore, the magnification needed to visualize the bound ice on the surface of low sample is approaching a degree in which the topographical changes of the sample forces the focus to be adequate only in a very distinct region.

Figure 15: Low level sample, overall assembly and magnification onto particle surface.

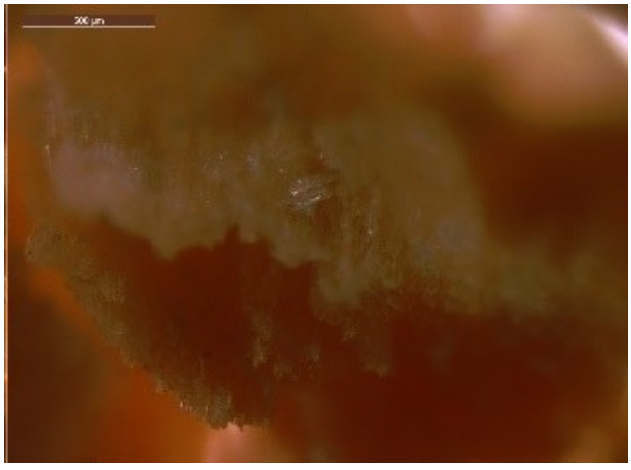

Figure 16: Low level sample, overall assembly and magnification onto particle surface.

With high level of moisture content frozen liquid bridges are visible. There is also considerable amount of ice droplets visible all over the particles. When examining length scale of the Figure 14 it is observed that the droplets and bridges have considerably larger dimensions than on the intermediate moisture content sample.

When these findings are compared against calculated statistical quantities some qualitative observations can be drawn. Emergence of liquid bridges correspond to sudden jump of variance of wet samples in Figure 9. The variance also seems to be growing moderately as amount of ice seen on the particle surfaces grows simultaneously. Same arguments apply to slope of skewness as described in section 4.4 and kurtosis of wet samples.

Figure 17: Intermediate level sample, overall assembly and magnification onto particle surface.

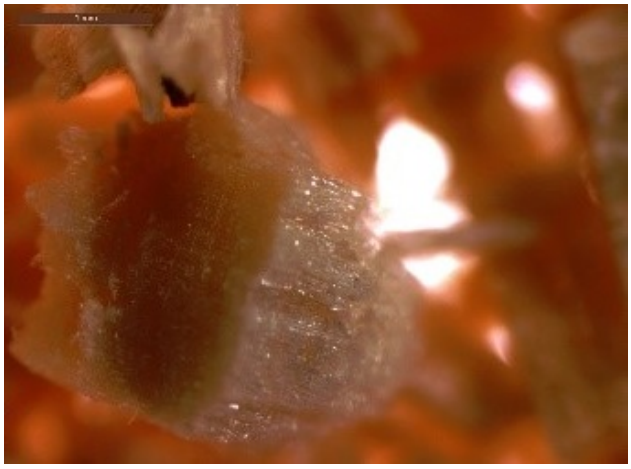

Figure 18: Intermediate level sample, overall assembly and magnification onto particle surface.

Last, the inspection reveals that the pendular state is with high probability the sole state in which the liquid water is present. This makes the strength of liquid bridging a monotonic function of liquid water available between particles as Delenne *et al.* [20] demonstrated in their simulations. Willet *et al.* [26] reached the similar results albeit with very simple configuration. From the control point of view this is fortunate as the drawback of calculated quantities here relied solely on the mechanisms of the granular system. Should the system extend to funicular region of liquid water state as moisture increases, the monotonicity might not be a valid assumption, as Delenne *et al.* [20] further point out. The assumption of the pendular state guarantees the presented statistical quantities to be in monotonic, one-to-one correspondence with liquid water content.

Figure 19: Overall assemblies of frozen and thawed high level samples. Bridges highlighted when presented as ice and liquid water, respectively.

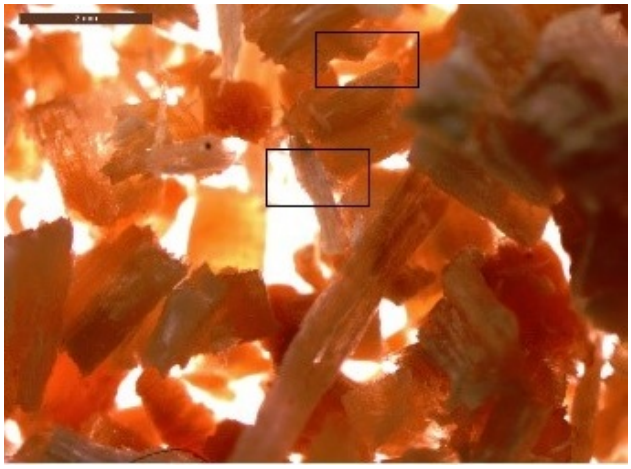

Figure 20: Overall assemblies of frozen and thawed high level samples. Bridges highlighted when presented as ice and liquid water, respectively.

4.7 Feasibility of inference method

The results presented are relying upon the phenomena of the liquid water present between saw dust particles. It remains to assess whether the observed statistically significant correlations yield inference of the moisture content in the sample since liquid water is also present inside the wood as described in section 2.

In section 2 it was concluded that bound liquid water is species specific, because this is dictated by the fiber saturation point. Variation between individual trees might, however, be present. Because saw dust originates from a sawmill cutting numerous trees with common species and growth environment, on average it may be assumed that individual variability is smoothed out because batches are

delivered in scale of tons. For the purposes of this study, then, the bound liquid water remains as a function of species only.

The amount of free liquid water that could be present in wood particles depends on the porosity and the pore size distribution. These are functions of species as described in section 2.

Because bound and free liquid water are seen as species dependent properties, it remains to show correlation between liquid water content and these variables. Here, it is plainly argued that bound and free water are monotonically increasing functions of total water. This seems logical because if this were not to hold, then adding liquid water to system could create "suction"; increasing interfacial liquid water content by injecting liquid water to sample would cause bound and/or free liquid water to be drawn out from the particles. Likewise, removing interfacial liquid water from sample by drying would cause particles to become more wet.

By these arguments, bound and free liquid water are monotonically increasing functions of total water. Delenne *et al.* [20] has asserted water content to be monotonically increasing function of water content. This is enough to show that one-to-one relationship between water content, bound water and free water must exist. Because there also exist one-to-one mapping between variance and water content, there must exist one-to-one mapping between moisture content and variance provided that the species of wood from which saw dust is derived stays constant. This makes the proposed inference method feasible.

5 Conclusion

The hypotheses made are consistent with observations in the experiments. Moreover, correlations between moisture content and phase of liquid water with calculated features were found. This can be asserted to the precision of the experimental design's capability to have eliminated all other sources of variation.

The physical source of correlation was deduced to be liquid interactions at the interface between particles by forming bridges. This becomes evident when comparing thawed samples with frozen samples. Thawed samples exhibit distinguishable correlations with statistical quantities but when dust freezes, these correlations disappear. Moreover, the statistical quantities behave similarly in thawed and frozen samples in low moistures. This is what one would expect to happen if the source of correlation is because of liquids at the interfaces; in low moisture contents the liquid water is not present in any form.

The findings of this work support the idea that a method using easily interpretable features to estimate moisture content is possible by classifying data via machine vision methods. The next stage of research would be the evaluation of cost effectiveness and verifying the estimation functionality with prolonged continuous feed times using the saw dust. Also, the features used were predecided with on the basis of experiences and observations made during preliminary laboratory work not reported here. This suggests that further improvements of inference could be made with more sophisticated methods, for example deep learning. Then, with the suggested set-up, the features would be learned directly from data. This seems interesting option as even the features pre-engineered in this work on the basis of human senses was successful.

References

[1] Islam MN, Narawi NA, Rosli R, Ali MH, Ani FN. 2018. Characterisation of biomass solid wastes for bio-fuel production in Brunei Darussalam. [web document] 7th Brunei International Conference on Engineering and Technology 2018, BICET 2018, 12 November 2018 through 14 November 2018, IET Conference Publications, Volume 2018, Issue CP750. DOI: https://doi.org/10.1049/cp.2018.1515.. Available at: https://ieeexplore.ieee.org/document/8726940 [cited 20.10.2019].

[2] Ma Y, Evans TM, Philips N, Cunningham N. Modeling the effect of moisture on the flowability of granular material. Meccanica. 2019;54(4-5):667–81.

[3] Tannous K, Lam PS, Sokhansanj S, Grace JR. Physical Properties for Flow Charaterization of Ground Biomass from Douglas Fir Wood. Particul Sci Technol. 2013;31(3):291–300.

[4] Ganesa V, Rosentrater KA, Muthukumarappan K. Flowability and handling characteristics of bulk solids and powders – a review with implications for DDGS. Biosyst Eng. 2008;101(4):425–35.

[5] Glass S, Zelinka S. Wood Handbook – Wood as Engineering Material, Centennial edition. Madison (WI): Forest Products Laboratory; 2010.

[6] Nyström J, Dahlquist E. Methods of determination of moisture content in woodchips for powerplants – a review. Fuel. 2004;83(7-8):773–9.

[7] Bureau S, Renard CM, Fakhjackh Z, Audergon JM. Infrared spectroscopy as a rapid tool to asses apricot fruit quality: comparison of two strategies for a model establishment. Acta Hortic. 2018;(1214):145–9.

[8] Skou, P. B., Berg, T. A., Aunsbjerg, S. D., Thaysen, D., Rasmussen, M. A. and van den Berg, F, 2017. Monitoring process quality using near infrared spectroscopy and partial least squares regression with prediction uncertainty estimation, Applied spectroscopy, Col 71, No 3, pp. 410-421.

[9] Nyström J, Thorin E, Backa SO. Dahlquist and E., 2005. Moisture content measurements on sawdust with radio frequency spectroscopy, Proceedings of the ASME Power Conference, Volume PART A, pp. 697-702. Chicago, IL, United States, 2005 ASME Power Conference.

[10] Lumay G, Boschini F, Train K, Bontempi S, Remy JC, Cloots R, *et al*. Measuring the flowing properties of powders and grains. Powder Technol. 2012;224:19–27.

[11] Rackl M, Grötsch F, Gunther W. 2017. Angle of repose revisited: When is heap a cone? [web document]. Published online: EDP Sciences. DOI: https://doi.org/10.1051/epjconf/201714002002. Available at: https://www.epjconferences.org/articles/epjconf/abs/2017/09/epjcof161726/epjconf161726.html [cited 29.10.2018].

[12] Tan Y, Gunther WA, Kessler S, Zhang L. 2017. Sample similarity analysis of angles of repose based on experimental results for DEM calibration. EPJ Web of Conferences, Vol 140, Article number 02026. Montpellier, France, 8th International Conference on Micromechanics on Granular Media, Powders and Grains. https://doi.org/10.1051/epjconf/201714002026.

[13] Jarray A, Magnanimo V, Luding S. Wet granular flow control through liquid induced cohesion. Powder Technol. 2019;341:126–39.

[14] Plinke MA, Maus R, Leith D. Experimental examination of factors that affect dust generation by using Heubach and MRI testers. Am Ind Hyg Assoc J. 1992 May;53(5):325–30.

[15] Zhao CF, Kryut N, Miller O. Capillary bridge force between non-perfectly wettable spherical particles: an analytical theory for pendular regime. Powder Technology, Col. 2018;339:827–37.

[16] Rezaei H, Jim Lim C, Lau A, Sokhansanj S. Size, shape and flow characterization of ground wood chip and ground wood pellet particles. Powder Technol. 2016;301:737–46.

[17] Louati H, Oulahna D, de Ryck A. Effect of the particle size and the liquid content on the shear behavior of wet granular material. Powder Technol. 2017;315:398–409.

[18] Iveson S, Beathe J, Page N. The dynamic strength of partially saturated powder compacts: the effect of liquid properties. Powder Technol. 2002;127(2):149–61.

[19] Althaus T, Windhab E. Characterization of wet powder flowability by shear cell measurements and compaction curves. Powder Technol. 2012;215-216:59–65.

[20] Delenne JY, Richefrey V, Farhang R. Capillary states of granular materials in the funicular state. AIP Conference Proceedings. New York: AIP Publishing; 2013. pp. 1023–6. 1542 pp.

[21] Plötze M, Niemz P. Porosity and pore size distribution of different wood types as determined by mercury intrusion porosimetry. Eur J Wood Wood Prod. 2011;69(4):649–57.

[22] Conners T. 2017. Distinguishing Softwoods from Hardwoods [web document]. Published online: Agricultural and Natural Resources Publications. FOR-125. Available at: https://uknowledge.uky.edu/anr_reports/105/?utm_ource=uknowledge.uky.edu%2Fanr_reports%2F105&tm_medium=PDF&utm_campaign=PDFCoverPages [citated 30.10.2018]

[23] Stasiak M, Molenda M, Banda M, Gondek E. Mechanical properties of saw dust and wood chips. Fuel. 2015;159:900–8.

[24] Al-Hashemi H, Al-Amoudi O. A review on the angle of repose of granular materials. Powder Technol. 2018;330:397–417.

[25] Geldart D, Abdullah EC, Hassanpour A, Nwoke LC, Wouters I. Characterization of powder flobability using measurement of angle of repose. China Particuology. 2006;4(3-4):104–7.

[26] Willet CD, Adams MJ, Johnson SA, Seville JP. Capillary bridges between two spherical bodies. Langmuir. 2001;16(24):9396–405.